Diamond-Based Capacitive Micromachined Ultrasonic Transducers in Immersion

Ahmet Murat Cetin and Baris Bayram, *Member, IEEE*

***Abstract*—Diamond is a superior membrane material for capacitive micromachined ultrasonic transducers (CMUTs). By using ultrananocrystalline diamond (UNCD) membrane and plasma-activated wafer bonding technology, a single diamond-based circular CMUT is demonstrated and operated in immersion for the first time. The diamond-based CMUT, biased at 100 V, is excited with a 10-cycle burst of 36 $V_{p\text{-}p}$ sine signal at 3.5 MHz. Pressure generated on a 2-D plane coincident with the normal of the CMUT is measured using a broadband hydrophone. Peak-to-peak hydrophone voltage measurements along the scan area clearly indicate the main lobe and the side lobes, as theoretically predicted by our directivity function calculations. The peak-to-peak hydrophone voltage on the axial direction of the CMUT is found to be in agreement with our theoretical calculations in the Fraunhofer region (-45 mm $< y < -15$ mm). The spectrum of the diamond-based CMUT is measured for a dc bias of 100 V, and ac excitation with 30-cycle bursts of 9, 36, and 54 $V_{p\text{-}p}$ sine signal. A peak response at 5.6 MHz is measured for all ac amplitudes. Overall, diamond is shown to be an applicable membrane for CMUT devices and applications.**

I. Introduction

Capacitive micromachined ultrasonic transducers (CMUTs) used in immersion are generally composed of vacuum-sealed cavities formed by membrane material [1]. The vacuum-sealed cavities are conventionally realized by two techniques. The first tchnique is the sacrificial release process, in which sacrificial material deposited before the membrane material is etched through the etch holes, and the etch holes are filled by deposition under low pressure to form the cavity [2]. The second technique is the direct wafer bonding method, in which two wafers (one having cavity patterning and the other having the membrane material) are bonded under elevated temperatures under vacuum [2].

Of these microfabrication methods, direct wafer bonding technology is more economical, offering better process control, higher yield, and more novelties in CMUT designs than the sacrificial release process [3]. Direct wafer bonding technology enabled development of single-crystal silicon membrane CMUTs rather than silicon nitride membrane CMUTs. Because the membrane and the substrate material are both silicon, direct wafer bonding at high temperatures (1100°C) is achieved without introducing any residual stress in the membrane [3]. Furthermore, IC-compatible direct wafer bonding at lower temperatures (400°C) can also be utilized [4]. Recently, successful flip-chip bonding of IC- and wafer-bonded 2-D CMUT arrays incorporating through-wafer trench-isolated interconnects has been demonstrated [5]. Therefore, recent developments allow the specifications of the CMUT design to be comfortably satisfied, facilitating the realization of industrial-grade CMUT products using direct wafer bonding technology [2].

Energy conversion efficiency of CMUTs has been of primary importance for ultrasound applications, and improvement of this efficiency has been extensively studied for ultrasound transducers [6], [7]. Conventionally, the CMUT is biased at a voltage below the collapse voltage, and an ac signal is applied to generate ultrasound [1]. The efficiency of the transducer is drastically improved as the bias voltage approaches the close vicinity of the collapse voltage [7]. However, this high efficiency comes with a risk of membrane collapse onto the substrate. Additionally, the ac amplitude is limited to a small excitation voltage around a large bias voltage to prevent membrane collapse during operation. Therefore, the maximum output pressure of a CMUT is inherently limited by the requirements of the conventional operation.

For potential applications such as high-intensity focused ultrasound (HIFU) in medical therapeutics, larger output pressures are essential. To offer unprecedented acoustic output pressure in transmit without the aforementioned limitations, novel CMUT operation modes of collapse [8] and collapse-snapback [9] were introduced. Both operation modes require the membrane to contact the substrate surface, which poses a problem for the durability of the membrane in terms of its structural integrity and tribological property. Large membrane deflection at collapse increases the stress within the membrane, and change of stress at ultrasound frequencies causes reduced lifetime and compromised reliability in these high-output-pressure operation modes.

Collapse-snapback mode requires the collision of the contacting surfaces every cycle, and heat released must be dissipated quickly to maintain stable operation. Based on the additional requirements of these modes to reach high output transmit pressure with a sustainable transducer operation, diamond is proposed as the ultimate solution for use as the membrane material. Mechanical (high Young's modulus, extreme hardness), thermal (large thermal conductivity, low thermal expansion coefficient),

Manuscript received March 10, 2011; accepted November 12, 2012. This work was supported by The Scientific and Technological Research Council of Turkey (TÜBİTAK) (PI: Baris Bayram, project numbers 107E153 and 110E072) and the Middle East Technical University (METU) (PI: Baris Bayram, project number BAP-08-11-2010-R-102).

Both authors were with the Department of Electrical and Electronics Engineering, Middle East Technical University, Ankara, Turkey, when this research was performed (e-mail: bbayram@metu.edu.tr).

DOI http://dx.doi.org/10.1109/TUFFC.2013.2578

TABLE I. PHYSICAL PARAMETERS OF THE DIAMOND-BASED CMUT.

Inner radius of the CMUT, μm	2586
Number of cells	2708
Center-to-center cell spacing (d_s), μm	94
Membrane diameter (d_m), μm	88
Electrode diameter (d_{Al}), μm	44
Electrode thickness (t_{Al}), μm	0.4
Diamond membrane thickness (t_m), μm	1.0
High temperature oxide thickness (t_{hto}), μm	0.23
Oxide and gap thickness (t_o), μm	1.57
Silicon substrate thickness (t_s), μm	525

and electrical properties (insulator, large electrical breakdown field) of diamond [10] are all in favor of its use in the microfabrication of CMUTs. Chemical inertness and biocompatibility are further benefits of diamond for CMUTs to be utilized in corrosive environments and biological samples, respectively [10].

Diamond is a perfect membrane material candidate based on its material properties. However, immature single-crystal diamond (SCD) deposition technologies have prevented integration of diamond membranes into CMUTs. Thin-film SCD-coated wafers are not commercially available for batch MEMS processes. Surface roughness of SCD is also high for use in CMUT microfabrication based on direct wafer bonding technology.

Recently, with improvements in diamond material growth and technology, ultrananocrystalline diamond (UNCD) was made commercially available as a thin film. UNCD shares many of the benefits of SCD with some compromised features, such as reduced resistivity resulting from graphitic forms enclosing polycrystalline diamond (SCD is an insulator, UNCD is highly resistive). A remarkable feature of UNCD as a membrane material is that it can be deposited as a thin film over a wafer surface with very low residual stress (i.e., <50 MPa). UNCD featuring smaller grain size and surface roughness has been recently explored for microelectromechanical systems (MEMS) applications such as RF MEMS resonators [11] and hybrid piezoelectric/UNCD cantilevers [12]. Recently, UNCD has also been used in the microfabrication of CMUTs with diamond membranes [13].

Microfabrication of CMUTs with diamond membranes [13] (such as UNCD)—especially if based on the plasma-activated wafer bonding technology [14], [15]—enables the utilization of key material properties of diamond, such as high Young's modulus, extreme hardness and large thermal conductivity [10], to improve the performance, reliability, and application range of CMUTs.

In this paper, a diamond-based CMUT is demonstrated and operated in immersion for the first time. Experimental characterization of the first-generation CMUT in immersion is performed for the conventional mode of operation using a broadband hydrophone in an ultrasound measurement system. Based on the 2-D pressure map of the CMUT, the main lobe and side lobes are experimentally identified and are verified with theoretical directivity calculations. The Fresnel and Fraunhofer regions of the single transducer are identified experimentally, and verified with theoretical diffraction calculations. The spectrum of the diamond-based CMUT is reported for different ac amplitudes in the conventional mode of operation.

The organization of this paper is as follows: Section II describes the single circular CMUT featuring diamond membranes used in this study. The details of the experimental setup using a broadband hydrophone are given in Section III. The results and analysis are presented in Section IV and discussed in Section V.

II. DEVICE DESCRIPTION

A single CMUT having a circular shape is designed with an inner radius of 2.6 mm. The mask design, prepared using commercially available software (L-EDIT, Tanner EDA, Monrovia, CA), is shown in Fig. 1(a). A 300-μm-wide ground disk encircles the inner structure. The transducer surface of the inner structure is composed of many circular cells [Fig. 1(b)]. Half metallization of the top electrode and cell-to-cell separation of 6 μm are used in the design. A cross-sectional drawing of the diamond-based CMUT is shown in Fig. 1(c). The physical dimensions of the CMUT are given in Table I. Circular cells are preferred in the microfabrication of the first diamond-based CMUTs in literature because of fast 2-D axisymmetric finite element modeling of these cells, with a trade-off in transducer fill factor and electromechanical coupling efficiency [7].

We fabricated the diamond-based CMUT used in this study. Microfabrication of CMUT with diamond membranes was made with 100-mm (4-in) wafers using plasma-

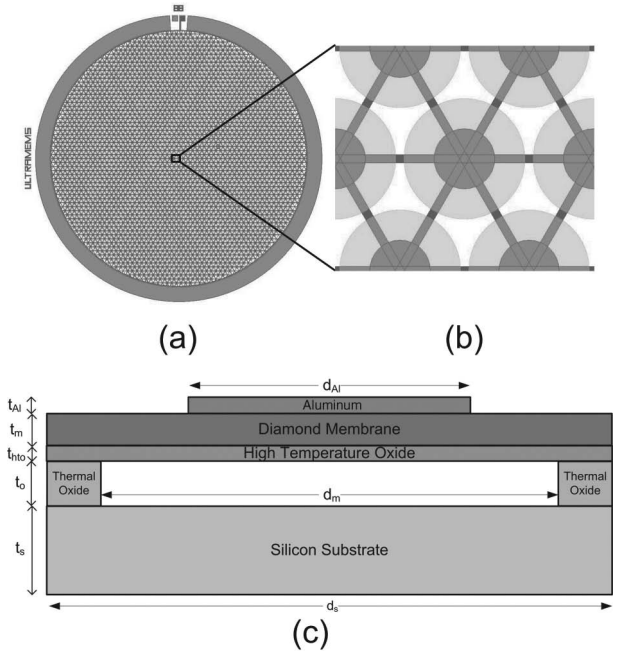

Fig. 1. A single CMUT design having a circular shape. (a) Top view of the single CMUT design. (b) Magnified, top view of a CMUT cell and its neighboring cells. (c) Schematic cross section of a CMUT cell.

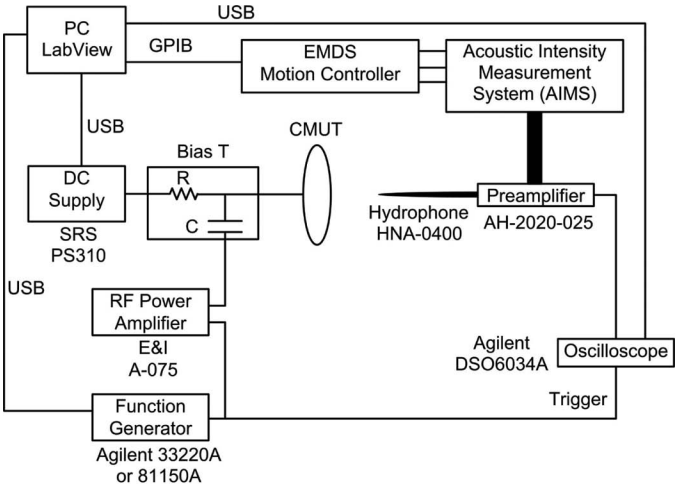

Fig. 2. Experimental setup used for acoustic field scan of the CMUT.

activated wafer bonding technology suitable for industrial grade mass production of CMUTs [13], [14]. The cavity was defined by lithography and reactive ion etching (RIE) of thermally grown oxide on n^+-doped silicon wafer. The membrane was prepared on a separate UNCD-coated silicon wafer with low-pressure chemical vapor deposition (LPCVD) and chemical mechanical polishing (CMP) of the high-temperature oxide (HTO). Both wafers were plasma-activated before wafer bonding [14]. To form the diamond membranes, the bulk silicon wafer of UNCD in the bonded pair was etched in tetramethylammonium hydroxide (TMAH), while the other side was protected by thermal oxide. The ohmic contact opening to n^+-doped silicon wafer was formed by plasma enhanced chemical vapor deposition of SiO_2, patterning via lithography, and etching of the SiO_2-UNCD-SiO_2 multilayer [13]. Aluminum (Al) was sputtered, patterned via lithography, and wet etched to form the top electrode on the membrane and the ground electrode on the n^+-doped silicon.

III. Experimental Setup

The acoustic pressure produced by a diamond-based CMUT was measured using the experimental setup in Fig. 2. The setup includes a dc supply (PS310, Stanford Research Systems, Sunnyvale, CA) and a function generator (33220A or 81150A, Agilent Technologies Inc., Santa Clara, CA) connected to an RF power amplifier (A-075, Electronics & Innovation Ltd., Rochester, NY) for biasing and driving the transducer, respectively. The dc and ac voltages are provided to a bias-T circuit connected to the CMUT. A broadband hydrophone (HNA-0400, Onda Corp., Sunnyvale, CA) connected to an immersible preamplifier (AH-2020–25, Onda Corp.) is placed in a motion-controlled stage in an ultrasound measurement system (AIMS, Onda Corp.). The output signal of the preamplifier is acquired by an oscilloscope (DSO6034A, Agilent Technologies Inc.), which is triggered by the function generator. All of these instruments are controlled and monitored by a PC running our ULTRASCAN program, based on a commercial software package (LabView, National Instruments Corp., Austin, TX). Communication with the instruments is handled by a commonly used object-oriented I/O language, VISA (Virtual Instrument Software Architecture).

The ultrasound measurement system features special hardware and software for positioning the hydrophone in 3 axes (x, y, z) with 11.1 μm resolution. ULTRASCAN communicates with AIMS through its software and functions exported through the installed dynamic-link libraries (DLLs). The data acquired by the oscilloscope has 1000 points for waveform snapshots in averaging mode. Our software can acquire data having a higher number of points by changing the time base and offset parameters automatically to receive multiple waveforms, and merging them as a single waveform.

IV. Results

Electrical impedance measurement of the CMUT is performed in air at a probe station using an impedance analyzer (4294A, Agilent Technologies Inc.). The impedance of the CMUT biased at 40 V is measured between 2 and 4 MHz frequency range, and resonance frequency of 2.8 MHz is observed in the experiment [Fig. 3]. Based on finite element modeling (FEM) using a commercially available software package (ANSYS, ANSYS Inc., Canonsburg, PA), resonance frequency of 3.3 MHz is calculated for the CMUT. A collapse voltage of 390 V is calculated using finite element analysis (FEA). The experimental and calculated collapse voltages are observed to be close, although a maximum dc voltage of 150 V is applied for this CMUT during the experiments. This is to protect the insufficiently thick and wide metallization of the top electrode over the diamond membrane from electrical failure.

The ultrasonic field generated by the diamond-based CMUT is measured in sunflower oil using a broadband

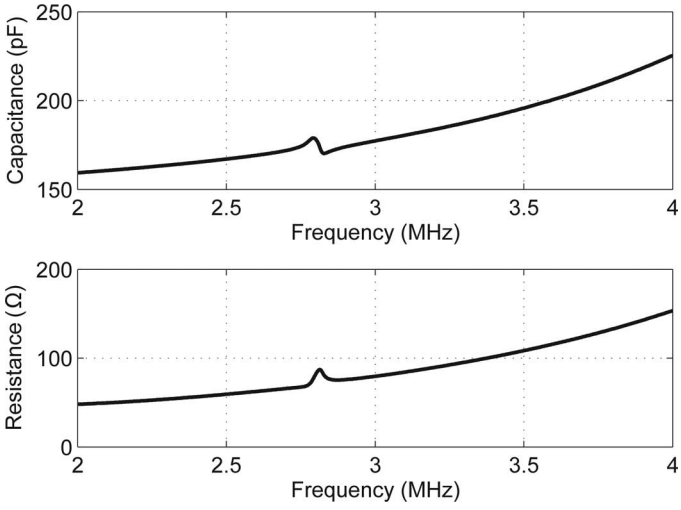

Fig. 3. Electrical impedance measurement (capacitance and resistance) of the CMUT in air at a bias voltage of 40 V.

$$D = \begin{cases} e^{-jkz} - \dfrac{2}{\pi\gamma^2}\displaystyle\int_{1-\gamma}^{1+\gamma} \sqrt{1-\left(\frac{1-\gamma^2+\xi^2}{2\xi}\right)} \times \exp\left[-jka\sqrt{\xi^2+\left(\frac{z}{a}\right)^2}\right] \mathrm{d}\xi, & \gamma \le 1 \\ \dfrac{e^{-jkz}}{\gamma^2} - \dfrac{2}{\pi}\displaystyle\int_{1-1/\gamma}^{1+1/\gamma} \sqrt{1-\left(\frac{1-\gamma^{-2}+\xi^2}{2\xi}\right)} \times \exp\left[-jka\sqrt{(\gamma\xi)^2+\left(\frac{z}{a}\right)^2}\right] \mathrm{d}\xi, & \gamma > 1 \end{cases} \tag{2}$$

hydrophone calibrated between 1 and 20 MHz. The hydrophone and the CMUT are aligned by making several initial hydrophone measurements [Fig. 4]. A minimum separation distance of 4.1 mm is selected to protect the hydrophone needle from mechanical damage. The CMUT, biased at 100 V, is excited with a 10-cycle burst of 36 $V_{p\text{-}p}$ sine signal at 3.5 MHz. The hydrophone scans the 2-D area with step sizes of 0.25 mm and 0.2 mm in x and y coordinates, respectively. The peak-to-peak hydrophone voltage is calculated using Matlab (The MathWorks Inc., Natick, MA) for the central zone of the received signal to remove the transient effects occurring in the initial and final parts of the 10-cycle burst [16]. The ULTRASCAN program adjusts the time base and offset of the oscilloscope to capture the received hydrophone signal automatically based on the time-of-flight calculations for the coordinates of the current scan location. Because measurement is performed over a 2-D scan area, some positions at specific angular positions will have no actual acoustic signal at all, making noise the dominant signal gathered at those positions. To suppress the noise level as much as possible, 4096 averages are taken during the measurement. Measurements of the peak-to-peak hydrophone voltage are shown for the 2-D scan area in Fig. 5. Assuming uniform particle velocity on the surface of a circular piston transducer mounted inside an infinite baffle, the pressure in the Fraunhofer region is given by [17]

$$p = \frac{j\rho_0 c_0 k a^2 v_0}{2r} e^{j(\omega t - kr)} \left[\frac{2J_1(ka\sin\theta)}{ka\sin\theta}\right], \tag{1}$$

where ρ_0 is the density of the medium, c_0 is the velocity of sound in the medium, k is the wave number, a is the radius of the transducer, v_0 is the amplitude of the surface velocity at an angular frequency of ω, r is the distance from the transducer center, θ is the angle with the transducer normal, and J_1 is the first-order Bessel function of the first kind. The directivity function, given in brackets of (1), specifies the pressure variation with direction [17]. The directions having zero pressure are calculated from the directivity function. Theoretical calculations of directions with null pressure response are superposed onto the pressure map of the CMUT in the experiments as straight lines on top of the measurement data [Fig. 5]. An excellent agreement for positioning of the main lobe and side lobes is observed between the measurement results and the theoretical calculations.

The peak-to-peak hydrophone signal at the center line of the CMUT ($x = 0$ mm) is extracted from the 2-D scan data, and presented in Fig. 6. The diffraction correction factor (D) [16] is calculated for the axial pressure of a circular piston transducer using an exact theoretical expression by (2), see above [18], where a is the radius of the transducer, b is the radius of the hydrophone, γ is the ratio of b over a, and z is the axial distance from the transducer center. The diffraction correction factor and the attenuation of sunflower oil [19] [$\alpha\,(\mathrm{dB/cm}) = 0.0647 \times f(\mathrm{MHz})^{1.85}$] are both considered in the calculation of the pressure variation in the axial direction of the transducer. A theoretical calculation of the pressure at the center line [from (2)] is plotted on top of the experimental work for comparison [16] (Fig. 6). Hydrophone radius of 200 μm [16] and attenuation (0.657 dB/cm at 3.5 MHz) of sunflower oil [19] are taken into account in the calculations. In the Fraunhofer region (-45 mm $< y < -15$ mm), an excellent match is observed between the measurement and the theory. In the Fresnel region (-15 mm $< y < 0$ mm), rapid interference maxima and minima is expected from the theory [17]. Because of the minimum separation distance of hydrophone and the CMUT, the measurement data are limited in the Fresnel region (-15 mm $< y <$ -4.1 mm). The experimental and theoretical minima coincide at $x = -8$ mm, although the normalized measured pressure (-6.3 dB) is not as low as the theoretical one (-23.4 dB). This is because the theoretical calculations are based on a circular piston transducer having uniform

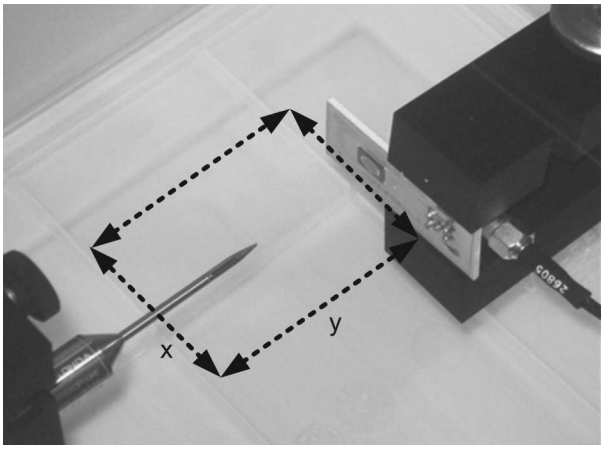

Fig. 4. Photo of aligned diamond-based CMUT and needle hydrophone in immersion. 2-D scan area in x and y coordinates are shown visually. The origin corresponds to the center of the CMUT.

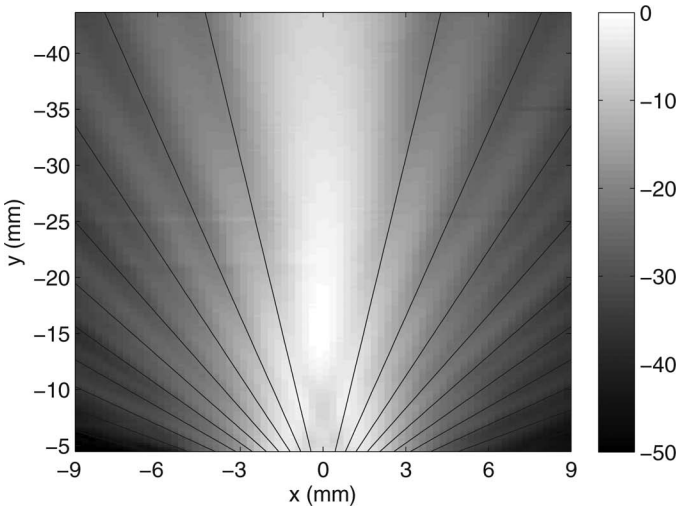

Fig. 5. Measurement results of the normalized peak-to-peak pressure (legend is in decibels) for the 2-D scan area. Theoretically calculated lines separating the main lobe and the side lobes are also shown on top of the measurement data.

displacement over the whole area, whereas the experimental results are taken with a CMUT having thousands of cells having nonuniform displacement (higher in the center, gradually decreasing to zero on the periphery of the cells) over the transducer surface. Nonuniform displacement profiles of each cell and rigid support regions between the neighboring cells cause pressure variation on the CMUT surface, which results in the observed near-field pressure characteristics in the Fresnel region.

Using the 2-D scan data and the calibration values of the hydrophone and the preamplifier, the acoustic output pressure is presented in Fig. 7 along the x-axis parallel to the CMUT surface at $y = 15$ mm [Fresnel distance ($S = 1$)], $y = 30$ mm ($S = 2$), and $y = 8.2$ mm ($S = 0.5$). A maximum pressure of 8.2 kPa is measured at the Fresnel distance at $x = 0$. A symmetrically spaced double peak at $S = 0.5$ and a single peak with a reduced pressure magnitude at $S = 2$ are measured, as expected by the theory [17].

The hydrophone is positioned at $y = -54.1$ mm along the normal of the CMUT. The CMUT, biased at 100 V, is excited with 30-cycle bursts of 9, 36, and 54 $V_{p\text{-}p}$ sine signal while the frequency of the signal is swept from 1 to 8 MHz with a step of 100 kHz (Fig. 8). A peak response at 5.6 MHz is measured for all ac amplitudes. A broadband response of the CMUT is observed except the dip observed at 4.2 MHz. This dip is caused by the electrical mismatch in the input port of the CMUT resulting from comparable series resistance and capacitance of the transducer. Although a higher acoustic output response is observed at 5.6 MHz, 3.5 MHz is used in the 2-D scan measurement to observe the pressure in the Fresnel and the Fraunhofer regions in our limited scan area. As the ac amplitude is increased from 9 $V_{p\text{-}p}$ to 54 $V_{p\text{-}p}$, an almost linear increase in pressure is observed, in agreement with the operation of the CMUT.

V. Discussion

The total capacitance of the diamond-based CMUT is calculated via FEM to be 89.4 pF for membranes, assuming the voltage of the top electrode extending over the full membrane. Highly resistive UNCD causes the actual half metallization to extend over a larger area electrically similar to other highly resistive membrane materials [6].

Because the peak membrane deflection is 8% of the gap height under only atmospheric pressure, and membrane capacitance is measured at approximately 10% of the collapse voltage, theoretical capacitance calculation should be a good estimation of the membrane capacitance. Comparison with the measured total capacitance (Fig. 3) reveals a parasitic capacitance as large as the membrane capacitance. Even more interesting is the increase of the

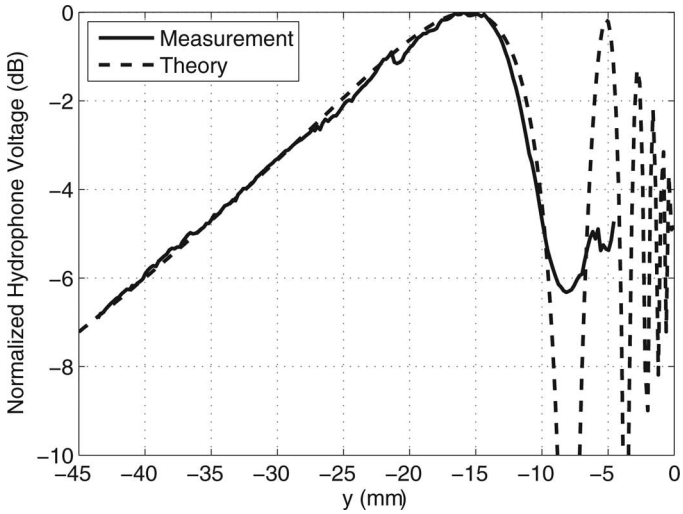

Fig. 6. Experimental and theoretical results of the normalized peak-to-peak pressure on the normal of the CMUT surface.

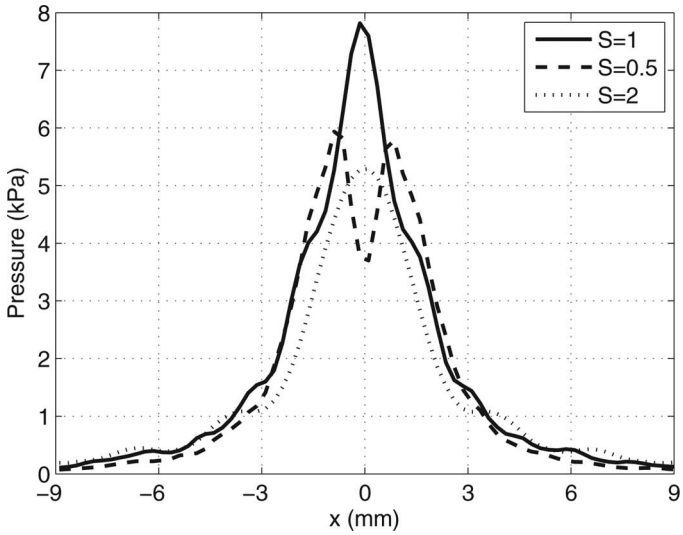

Fig. 7. Experimental acoustic output pressure along the x-axis parallel to the CMUT surface at $y = 15$ mm [Fresnel distance ($S = 1$)], $y = 30$ mm ($S = 2$), and $y = 8.2$ mm ($S = 0.5$).

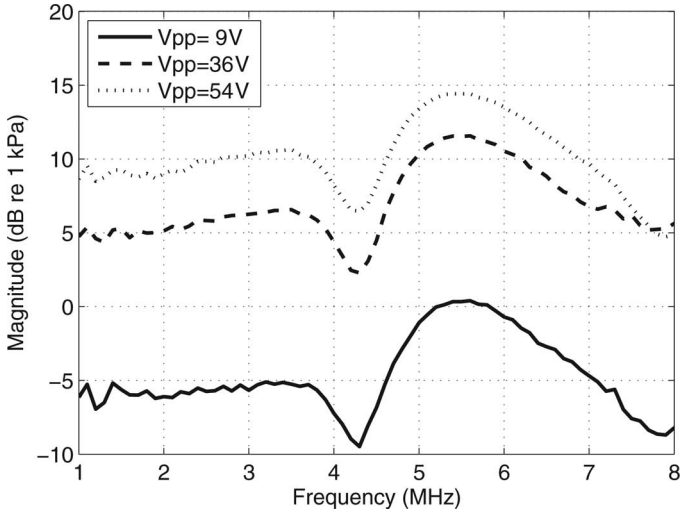

Fig. 8. Spectrum of the diamond-based CMUT in conventional operation. The CMUT is biased at 100 V. Peak-to-peak amplitudes of 9, 36, and 54 V are used for ac excitation.

capacitance from 160 pF at 2 MHz to 225 pF at 4 MHz, whereas the series resistance increases from 50 Ω at 2 MHz to 150 Ω at 4 MHz. The silicon substrate and the undoped diamond are resistive enough to cause series resistance comparable to the capacitance of the CMUT. Although half metallization is used to reduce parasitics, assuming the undoped diamond to act like an insulator, the slightly graphitic nature of the UNCD makes it electrically resistive rather than an insulator, and the electrical behavior of the membrane becomes quite complex at the frequency of interest. This electrical problem causes the electrical mismatch of the transducer in transmit, reducing the signal coupling to the capacitance of the CMUT at 4.2 MHz. This mismatch suggests that higher quality deposition of diamond promises to improve device performance.

When the CMUT is biased at 100 V, a leakage current of 0.08 mA is supplied by the dc supply. High leakage current is an indication of the high parasitic capacitance formed by the silicon dioxide support regions of the circular membranes. However, the thickness and the width of the metal lines are initially selected for half metallization over an insulating diamond membrane. With the conductive nature of UNCD, the capacitance is larger than considered. Higher bias voltages are avoided to protect the metallization of the top electrode from electromigration under high current densities, particularly over the thin metal line connecting the pad electrode to the metal on circular cells. Higher voltages up to the collapse voltage could be applied without the membrane collapse and the electrical breakdown of the silicon dioxide if the metallization were sufficiently thick and wide.

It should be noted that high parasitics and limited dc voltage observed in this device are not inherent problems of the diamond membrane. Basically, a revised CMUT design taking the resistivity of UNCD into account should not suffer from any of these problems, and will be essentially operable not only under high dc voltages in the conventional mode but will also be qualified for collapse and collpase-snapback modes of operation.

The experimental setup in [Fig. 2] is a strong platform for performing precise and reliable acoustic scanning measurements. The most sensitive and vulnerable part of the system is the hydrophone. The hydrophone is broadband so it is able to receive signals from all angles, and it is calibrated from 1 to 20 MHz. The hydrophone is of the needle type, causing very low field disturbance. It is a commercially available hydrophone developed for high-intensity ultrasound field measurements. The 2-D scan data presented in Fig. 5 was collected in 22 h because 4096 waveforms were averaged for each scan location.

In all hydrophone measurements, sufficient delay of the received signal is provided for pressure mapping in the Fresnel region so that the actual acoustic signal will not be affected by the electromagnetic interference picked up by the hydrophone for high burst counts.

A broadband response of the CMUT is observed except the dip observed at 4.2 MHz. Reduced pressure output at 4.2 MHz is an indication of the electrical impedance mismatch explained earlier. Because of the comparable values of real and imaginary impedances around 4 MHz, the electrical impedance mismatch causes a 5 dB loss in the transmit pressure. Employing full metallization and increasing the number of pad electrode connections to overcome electromigration are two solutions to overcome this mismatch problem.

This first CMUT biased at 25% of the collapse voltage provides an electromechanical coupling efficiency of 0.02 [8]. A large gap separation of 1.57 μm, high parasitic capacitance, and inadequate metallization over resisitive UNCD were identified as the limiting factors of output acoustic pressure. This study is the first experimental demonstration and characterization of the very first generation diamond-based CMUT in immersion. We showed that diamond-based CMUTs can be realized, reported their operational characteristics, and identified the current limitations. Improving the device performance will be the objective of future work involving further diamond deposition improvements and its characterization, and improved CMUT designs based on first-generation CMUT results.

VI. Conclusion

The diamond-based single CMUT fabricated with plasma-activated wafer bonding technology was operated in immersion for the first time. Fresnel and Fraunhofer regions of the CMUT were experimentally characterized in sunflower oil and are in agreement with theory. Theoretical calculations of directivity and diffraction of a circular piston transducer were used to verify the proper immersion operation of the first diamond-based single CMUT having thousands of cells. The experimental field pattern verified by the theoretical calculations showed the immersed operation and high yield for our CMUTs with

diamond membranes. We have reported the operational characteristics of the first diamond CMUT and identified the key challenges for improving these devices.

Acknowledgments

This work was supported by The Scientific and Technological Research Council of Turkey (TÜBİTAK) (PI: Baris Bayram, project no: 107E153, 110E072). This work was conducted in the cleanroom facility of the METU MEMS Center (Middle East Technical University, Ankara, Turkey). The authors thank Advanced Diamond Technologies for providing very-low-stress UNCD DOI wafers, D. Trojan from Axus Technology for performing CMP on the wafer surfaces of high-temperature oxide on DOI wafers, and A. Filbert from EVGroup for performing EVG301 wafer cleaning, EVG810LT plasma activation, and EVG520IS wafer bonding.

References

[1] H. T. Soh, I. Ladabaum, A. Atalar, C. F. Quate, and B. T. Khuri-Yakub, "Silicon micromachined ultrasonic immersion transducers," *Appl. Phys. Lett.*, vol. 69, no. 24, pp. 3674–3676, 1996.

[2] A. S. Ergun, Y. Huang, X. Zhuang, O. Oralkan, G. G. Yaralioglu, and B. T. Khuri-Yakub, "Capacitive micromachined ultrasonic transducers: Fabrication technology," *IEEE Trans. Ultrason. Ferroelectr. Freq. Control*, vol. 52, no. 12, pp. 2242–2258, 2005.

[3] Y. Huang, A. S. Ergun, E. Haeggstrom, M. H. Badi, and B. T. Khuri-Yakub, "Fabricating capacitive micromachined ultrasonic transducers with wafer-bonding technology," *J. Microelectromech. Syst.*, vol. 12, no. 2, pp. 128–137, 2003.

[4] A. Berthold and M. J. Vellekoop, "IC-compatible silicon wafer-to-wafer bonding," *Sens. Actuators A*, vol. 60, no. 1–3, pp. 208–211, 1997.

[5] X. Zhuang, I. O. Wygant, D. S. Lin, M. Kupnik, O. Oralkan, and B. T. Khuri-Yakub, "Wafer-bonded 2-D CMUT arrays incorporating through-wafer trench-isolated interconnects with a supporting frame," *IEEE Trans. Ultrason. Ferroelectr. Freq. Control*, vol. 56, no. 1, pp. 182–192, Jan. 2009.

[6] A. S. Ergun, G. G. Yaralioglu, O. Oralkan, and B. T. Khuri-Yakub, *Techniques and Applications of Capacitive Micromachined Ultrasonic Transducers, MEMS/NEMS Handbook V2—Fabrication Techniques for MEMS/NEMS*. New York, NY: Springer, 2005.

[7] G. G. Yaralioglu, A. S. Ergun, B. Bayram, E. Haeggstrom, and B. T. Khuri-Yakub, "Calculation and measurement of electromechanical coupling coefficient of capacitive micromachined ultrasonic transducers," *IEEE Trans. Ultrason. Ferroelectr. Freq. Control*, vol. 50, no. 4, pp. 449–456, Apr. 2003.

[8] B. Bayram, E. Hæggström, G. G. Yaralioglu, and B. T. Khuri-Yakub, "A new regime for operating capacitive micromachined ultrasonic transducers," *IEEE Trans. Ultrason. Ferroelectr. Freq. Control*, vol. 50, pp. 1184–1190, Sep. 2003.

[9] B. Bayram, Ö. Oralkan, A. S. Ergun, E. Hæggström, G. G. Yaralioglu, and B. T. Khuri-Yakub, "Capacitive micromachined ultrasonic transducer design for high power transmission," *IEEE Trans. Ultrason. Ferroelectr. Freq. Control*, vol. 52, no. 2, pp. 326–339, Feb. 2005.

[10] V. Ralchenko, T. Galkina, A. Klokov, A. Sharkov, S. Chernook, and V. Martovitsky, in *Science and Technology of Semiconductor-On-Insulator Structures and Devices Operating in a Harsh Environment*, D. Flandre, A. N. Nazarov, P. L. F. Hemment, Eds., Dordrecht, The Netherlands: Springer, 2005, p. 77.

[11] S. Pacheco, P. Zurcher, S. Young, D. Weston, W. Dauksher, O. Auciello, J. Carlisle, N. Kane, and J. Birrell, "Characterization of low-temperature ultrananocrystalline diamond RF MEMS resonators," in *Proc. 35th European Microwave Conf.*, 2005, pp. 1523–1526.

[12] S. Srinivasan, J. Hiller, B. Kabius, and O. Auciello, "Piezoelectric/ultrananocrystalline diamond heterostructures for high-performance multifunctional micro/nanoelectromechanical systems," *Appl. Phys. Lett.*, vol. 90, no. 13, art. no. 134101, 2007.

[13] B. Bayram, "Diamond-based capacitive micromachined ultrasonic transducers," *Diam. Relat. Mater.*, vol. 22, no. 2, pp. 6–11, Feb. 2012.

[14] B. Bayram, O. Akar, and T. Akin, "Plasma-activated direct bonding of diamond-on-insulator wafers to thermal oxide grown silicon wafers," *Diam. Relat. Mater.*, vol. 19, no. 11, pp. 1431–1435, Nov. 2010.

[15] B. Bayram, "Fabrication of SiO_2-stacked diamond membranes and their characteristics for microelectromechanical applications," *Diam. Relat. Mater.*, vol. 20, no. 4, pp. 459–463, Apr. 2011.

[16] A. Goldstein, D. R. Gandhi, and W. D. O'Brien, "Diffraction effects in hydrophone measurements," *IEEE Trans. Ultrason. Ferroelectr. Freq. Control*, vol. 45, no. 4, pp. 972–979, Jul. 1998.

[17] J. D. N. Cheeke, *Fundamentals and Applications of Ultrasonic Waves*. Boca Raton, FL: CRC Press, 2002, ch. 6.

[18] K. Beissner, "Exact integral expression for the diffraction loss of a circular piston source," *Acustica*, vol. 49, no. 3, pp. 212–217, 1981.

[19] R. Chanamai and D. J. McClements, "Ultrasonic attenuation of edible oils," *J. Am. Oil Chem. Soc.*, vol. 75, no. 10, pp. 1447–1448, 1998.

Ahmet Murat Cetin was born in Uskudar, Turkey. He received the B.S. degree in 1998 from Gazi University, Ankara, Turkey, and the M.S. degree from the Middle East Technical University, Ankara, Turkey, in 2011; both degrees were in electrical engineering.

His research interests include design and characterization of capacitive micromachined ultrasonic transducers (CMUTs).

Baris Bayram was born in Izmir, Turkey. He received the B.S. degree in 2000 from Bilkent University, Ankara, Turkey, and the M.S. and Ph.D. degrees in 2002 and 2006, respectively, from Stanford University, Stanford, CA; all degrees were in electrical engineering. From 2000 to 2006, he was a Research Assistant at E. L. Ginzton Laboratory, Stanford University, where he worked with Prof. Khuri Yakub—the inventor of capacitive micromachined ultrasonic transducers (CMUTs). Since 2006, he has pursued his academic career at the Middle East Technical University, Ankara, Turkey, where he is currently a tenure-track Assistant Professor. In 2012, he received the title of Associate Professor from the Higher University Council of Turkey.

He is the director of the ULTRAMEMS Research Laboratory in the Department of Electrical and Electronics Engineering at the Middle East Technical University, Ankara, Turkey. His research interests include design, microfabrication, and characterization of capacitive micromachined ultrasonic transducers (CMUTs). He is the inventor of and investigates the nonlinear operation regimes (collapsed and collapse-snapback) of CMUTs for high acoustic output performance and better crosstalk performance, and explores the unique potential advantages of diamond-based MEMS devices for biomedical applications. His current research mainly focuses on nanocrystalline diamond as a novel membrane material for microfabrication of CMUTs for high-power applications under harsh operating conditions, and IC–MEMS integration for power-efficient, robust operation.

He is the recipient of the 2011 Young Scientists Award Programme (GEBIP) of The Turkish Academy of Sciences (TÜBA) in the field of electrical and electronics engineering for his pioneering work on micro electromechanical systems (MEMS), ultrasound, and diamond-based capacitive micromachined ultrasonic transducers. He has (co-)authored 12 journal and 14 conference papers, and has been issued 2 U.S. patents. He is a member of the Acoustical Society of America (ASA), the IEEE, and the IEEE Ultrasonics, Ferroelectrics, and Frequency Control (UFFC) Society.